PennState College of Engineering

ESM Engineering Science and Mechanics

ESM TODAY 2023

March 18, 2023
1st Floor Lobby Leonhard Building

Photo courtesy of Rahul Pendurthi, 2022 ESM Today Art-in-Science Winner

20th Annual Engineering Science and Mechanics Research Symposium

Table of Contents

ESM Today 2023 organized by:

Olivia Cook

Lovejoy Mutswatiwa

Nailah Oliver

Flor Parra

Dipanjan Sen

Schedule of Events

8:30 AM – 9:00 AM	**Registration**
9:00 AM – 9:30 AM	**Departmental Address by Dr. Meunier**
9:30 AM – 9:45 AM	**Break**
9:45 AM – 12:00 PM	**Oral Presentations Rooms 101, 102, 103, 202, 203**
12:00 PM – 1:00 PM	**Lunch EES Building***
1:00 PM – 2:00 PM	**Poster Presentations & Art-in-Science Exhibition**
2:00 PM – 2:45 PM	**Safety Olympics**
2:45 PM – 3:00 PM	**Awards Ceremony**

*Please note that lunch will be provided in 215 EES and you are free to gather in the conference rooms (207A & 216 EES) and common areas of the building to eat before returning for the poster session.

Participants Lists and Abstract Titles

Oral Presentations

Oral Presentations			
Speaker	**Abstract Title**	**Speaker**	**Abstract Title**
Advanced Materials, Technologies, and Devices			
Andrew Pannone	*Machine Learning-Aided Non-Functionalized Graphene Chemitransistors for Highly Selective Chemisensing in Liquid Media*	Darsith Jayachandran	*Monolithic three-dimensional (3D) integration of two-dimensional (2D) field effect transistors*
Dipanjan Sen	*An On-chip True Random Number Generator Based on Atomically Thin Two-dimensional Materials*	Federico Krauch	*Optimization and implementation of dielectric resonator couplings in MRI applications to increase the transmit signal*
Harikrishnan Ravichandran	*Acceleration of Noise-immune Spiking Neural Network using Stochastic Defect Dynamics in Atomically Thin Transistors*	Mayukh Das	*An Atomically Thin, Ferromagnetic, Photosensitive, and Programmable Vanadium Disulfide Memtransistor*
Mecit Altan Alioglu	*3D Embedded Printing of Microfluidic Devices using a Functional Silicone Composite Support Bath*	M. Jahangir Khan Lodhi	*In-situ Transmission electron microscopy to unravel complex corrosion mechanisms*
Muhtasim Ul Karim Sadaf	*A Bio-inspired Visuotactile Neuron for Multisensory Integration*	Najam Sakib	*Ultra-scaled Contacts to Monolayer MoS_2 Field Effect Transistors*
Subir Ghosh	*An All 2D Bio-inspired Gustatory Circuit for Mimicking Physiology and Psychology of Feeding Behavior*	Thomas Schranghamer	*Gamma Radiation Resilience of Two-Dimensional Electronics based on MoS_2*
Yikai Zheng	*Graphene Strain-effect Transistor with Colossal ON/OFF Current Ratio Enabled by Reversible Nano-crack Formation in Metal Electrodes on Piezoelectric Substrates*	Zhiyu Zhang	*Comprehensive Comparison of the Full-cascade and Quick Calculation Modes in the Monte Carlo Simulation of Ion Irradiation Damage in Monoatomic Targets*

Mechanics of Materials			
Arnab Chatterjee	*Additive Manufacturing build plan dependence of spatially resolved structure-behavior relations in active materials*	Avery Brown	*Compression Buckling of Carbon/Epoxy Panels with Noise-Reducing T-Stiffeners*
Dingchuan Xue	*Phase field modeling of dendrite growth and crack propagation in solid electrolytes*	Haley Jones	*Ultrasonic Evaluation of Cold Sintered ZnO: Investigating Effects of Transient Phase and Heating Rate in Microstructure*
Zhu Yingxin	*Bandgap Modulation of ZnO Nanowires through Elastic Strain Engineering*		

Dynamic Systems, Acoustics, and Vibrations			
Caeden Smith	*Noninvasive Characterization of Solidification Mushy Zones Using Ultrasound*	Cate Rollins	*Ultrasonic Nondestructive Evaluation in Thin Materials Using Finite Elements*
Daniel Giraldo Guzman	*Surface and plate wave propagation control using topology-optimized metasurfaces*	Evan Bozek	*Reconstructing the Internal Vibration Response of Jet Engines from External Sensors using Elastic Net Regression*
Lalith Sai Srinivas Pillarisetti	*Controlling surface waves in granular media at seismic frequencies using a meta-barrier*	Michail Skiadopoulos	*Porosity quantification of metallic components based on synthetic ultrasonic signals using Deep Learning*
Pavan Kumar	*General Solution for a Single-Phase Conduction Problem of a Finite-Slab with a Growing or Receding Boundary*	Prabhav Borate	*Predicting laboratory-scaled shear failure from time-lapse active source ultrasonic data using a physics-informed neural network (PINN) model*
Vaibhav Pal	*High-throughput microgel fabrication via air-assisted co-axial jetting for cell encapsulation, 3D bioprinting, and scaffolding applications*	Lauren Katch	*A ray tracing approach to focusing ultrasonic beams in isotropic and anisotropic solids*

Optoelectronics, Photonics, and Lasers			
Nailah Oliver*	*Temperature mapping for superconducting radio-frequency cavities using type-II fiber Bragg grating sensors*	Ricardo Fiallo	*Alteration of Optical Bragg Phenomenon by Substrate Roughness*

Emerging Manufacturing Processes			
Anubhav Roy	*Influence of higher order scattering in estimates of ultrasonic attenuation in complex metals*	Christopher Wheatley Jr.	*Ultrasonic nondestructive characterization of cold sintered dielectric microstructures at various scales*
Colin Williams	*Towards a Multiscale Approach to Model Nonlinear Wave Propagation for Characterization of Metallic Components*	Grant Klinger	*A Piecewise Approach to Solving the Thermal Inverse Problem*
Irem Deniz Derman	*High-Throughput Bioprinting of the Nasal Epithelium using Patient-derived Nasal Epithelial Cells*	Lovejoy Mutswatiwa	*High-speed synchrotron x-ray imaging of micro-scale cavitation in laser-generated molten melt pools*

*Multiple specialty areas are associated with the presentation.

Oral Presentation Schedule

Time	Room 101	Room 102	Room 103	Room 202	Room 203
	Presenters				
9:45 AM – 10:00 AM	Dipanjan Sen	Pavan Kumar	Colin Williams	Haley Jones	Lauren Katch
10:00 AM – 10:15 AM	Dingchuan Xue	Andrew Pannone	Avery Brown	Grant Klinger	Harikrishnan Ravichandran
10:15 AM – 10:30 AM	Caeden Smith	Cate Rollins	Darsith Jayachandran	Evan Bozek	Thomas Schranghamer
10:30 AM – 10:45 AM	Federico Krauch	Arnab Chatterjee	Michail Skiadopoulos	Anubhav Roy	Irem Deniz Derman
10:45 AM – 11:00 AM	**Break**				
11:00 AM – 11:15 AM	Prabhav Borate	Mayukh Das	Ricardo Fiallo	Muhtasim Ul Karim Sadaf	Mecit Altan Alioglu
11:15 AM – 11:30 AM	Nailah Oliver	Christopher Wheatley Jr.	Daniel Giraldo Guzman	Yikai Zheng	Lovejoy Mutswatiwa
11:30 AM – 11:45 AM	Najam Sakib	Zhu Yingxin	M. Jahangir Khan Lodhi	Vaibhav Pal	Lalith Sai Srinivas Pillarisetti
11:45 AM – 12:00 PM	Zhiyu Zhang				

Machine Learning-Aided Non-Functionalized Graphene Chemitransistors for Highly Selective Chemisensing in Liquid Media

Andrew Pannone, Jackson Paul Robbins, Akshay Wali, Dipanjan Sen, Michael B. Felins, and Saptarshi Das

The development of highly selective and miniaturized chemisensors for liquid media can enable new discoveries and empower a wide range of disciplines from biology to human health, marine ecology to climate change, and industrial process monitoring to food safety. While the two-terminal chemiresistor architecture has been remarkably successful in this regard, it relies on appropriate surface functionalization to achieve selectivity for a specific target analyte. Furthermore, sensor drift and sensor-to-sensor variation present in multiplexed chemisensor arrays can severely impact their reliability and obscure the response of individual sensors to the target analytes. We overcome these challenges by introducing a new sensing paradigm that integrates an array of three-terminal chemitransistors based on monolayer graphene with an ensemble of machine learning (ML) algorithms. The extraordinary transport properties of graphene combined with its electrochemically inert basal plane allow a wide range of chemical species to electrostatically control the channel conductivity in a liquid medium through voltage gating. This in turn expands the parameter space for the sensing elements which enables the integration of various unsupervised and supervised ML algorithms to eliminate the need for surface functionalization, eradicate the need for sensor calibration, and minimize the impact of sensor-to-sensor variation. Our ML-aided, non-functionalized, and reusable graphene chemitransistors were found to be highly selective to de-ionized (DI) water, multiple chloride salts including NaCl, LiCl, $CaCl_2$, and $MgCl_2$ that are relevant to biosensing, several weak acids including acetic, propionic, and citric acid that are used in the food industry, as well as more complex solutions and processes such as decaying juices extracted from different fruits (grape, orange, watermelon, and pineapple).

Influence of higher order scattering in estimates of ultrasonic attenuation in complex metals

Anubhav Roy and Christopher M. Kube

Science and technology have evolved with diverse applications of engineering materials over the decades. Both cost and mechanical complexity associated with manufacturing have increased accordingly. For example, the high cost associated with additively manufactured (AM) metals can be mitigated by integrating an efficient nondestructive evaluation (NDE) setup with the manufacturing process. Thus, it is essential to accurately understand how stress waves interact and scatter while propagating through polycrystalline metals consisting of heterogeneities in the microstructure. The existing analytical model involving first-order smoothing approximation (FOSA) provides accurate estimates of wave speed and attenuation in some low-scattering metals over a wide range of ultrasonic frequencies. However, mechanical complexity is a barrier to understanding the behavior of complex metals containing pores, defects, or texture. Unexpected discrepancies have been reported between the estimates from the FOSA-based model and the more realistic finite-element (FE) model for various metals. This discrepancy between the attenuation predictions reaches as high as 70% for highly anisotropic metals like Lithium, even for low ultrasonic frequencies. On the other hand, computational inefficiency restricts the FE-based models from being incorporated into the NDE setups. Thus, for the first time, the current research aims to introduce the third-order smoothing approximation (TOSA) in the existing FOSA-based

analytical model for a more accurate yet efficient prediction of ultrasonic scattering in complex metals. Results from the current TOSA-based model at low frequencies indicate up to 2% and 3.5% improvement in longitudinal and transverse attenuation estimates for some metals comprised of highly anisotropic crystallite grains. The current effort includes extending the model to high frequencies where the improvement is expected to be fully effective.

Additive Manufacturing build plan dependence of spatially resolved structure-behavior relations in active materials

Arnab Chatterjee and Reginald Felix Hamilton

Active materials are a new class of material systems that undergo a reversible shape change under external stimuli. Shape Memory Alloys (SMAs) are a class of active materials. In this work, we fabricated Nickel-Titanium based SMAs using Additive Manufacturing (AM). AM is a layer-by-layer manufacturing technique that allows customizing extrinsic size and shape along with intrinsic composition and structure. Laser Directed Energy Deposition (LDED) technique employs pre-blended elemental powder feedstock for controlling SMA composition. As a result of layer/pass wise buildup, the intrinsic factors will vary spatially. Since it is generally accepted that a spatially uniform composition and structure are essential for optimal SMA behavior, varying the AM build plan has been explored in this work for reducing heterogeneity inherent to AM. Two build plans differentiated by the orientation of the tool path with respect to the mechanical loading direction are manufactured. The signatures of layer/pass wise overlapping regions along various build planes have been observed. Microstructural hierarchy and behavior have been spatially investigated along these signatures in locations corresponding to build parameters. Along different planes, the grain morphology varies between equiaxed grains with higher aspect ratio and elongated grains with low aspect ratio. The build plan having higher number of layers have predominant eutectic morphology of second phase along its plane, whereas one having higher number of passes have varying morphologies. The microhardness increases along build direction and along the laser scan direction, it falls from near free edge to the center of the builds. Thus, combined study of X-Ray Diffraction, microscopy, and microhardness can successfully produce spatial maps to demonstrate a local structure-behavior relations to assess impact of AM build plans.

Compression Buckling of Carbon/Epoxy Panels with Noise-Reducing T-Stiffeners

Avery Brown, Anna Moorhouse, Charles Bakis, Edward Smith, Benjamin Beck, and Micah Shepherd

Aircraft are typically constructed using stiffened thin-walled structural elements that are increasingly being made of carbon fiber reinforced epoxy composites because of their high strength and stiffness per unit weight. Certain types of aircraft, such as rotorcraft, have high levels of interior noise generated by the vibration of the stiffened panels, which can cause discomfort and hearing damage in the passengers and crew. In the current work, it is hypothesized that interior noise can be reduced by incorporating a novel type of noise reduction known as the “acoustic black hole” into the stiffeners of stiffened carbon/epoxy panels. The acoustic black hole concept entails tapering the thickness of the stiffener as the free edge is approached so that vibrations within the stiffener can be extinguished at the free edge with a light-weight damping material. This investigation aims to characterize the axial compressive buckling and post-buckling behavior of a carbon/epoxy panel with T-shaped stiffeners with and without an acoustic black hole thickness

taper molded into the stem of the "T". Numerical calculations were carried out using the finite element software Abaqus to predict buckling and post-buckling loads and mode shapes. Compressive buckling tests were conducted to measure the buckling and post-buckling load-displacement and load strain relationships, as well as the collapse load and associated failure mode. Full field strain and displacement were measured using the three-dimensional digital image correlation method. Finite element predictions for the first buckling mode shape and initial structural stiffness showed good alignment with the experiments. Post-buckling numerical modeling did not show excellent agreement with the experimental results. Experimental results indicated significantly more local stiffener displacement for the power-law tapered stiffener design versus the non-tapered design, but no reduction in the collapse load. Failure of the panels was typically associated with debonding between the stiffeners and skin.

Noninvasive Characterization of Solidification Mushy Zones Using Ultrasound

Caeden Smith, Lauren Katch, and Andrea P. Argüelles

Solidification is a fundamental physical process present in manufacturing techniques ranging from casting to additive manufacturing. Many material defects may form as a liquid solidifies, including cracks, voids, and porosity. Therefore, much research has been devoted to predicting defect formation during solidification. To this end, numerical simulations show a strong relation between the properties of a region at the liquid-solid interface of a solidifying material known as the mushy zone and defect formation. In this study, an acoustic model for ultrasonic reflections from a continuous matching layer is applied to the mushy zone. The model was successfully validated using an elastic simulation in Abaqus. Further testing is necessary to recreate these results experimentally. This work makes progress towards enabling noninvasive characterization of the mushy zone using ultrasound with the goal of real-time defect detection and prediction.

Ultrasonic Nondestructive Evaluation in Thin Materials Using Finite Elements

Cate Rollins, Lauren Katch, and Andrea P. Argüelles

The ability to detect and size back surface-breaking flaws is key to preventing catastrophic part failures. Ultrasonic nondestructive testing can be used to detect back surface-breaking flaws, but thin materials still present challenges. This presentation explores a method for improving the detection of small back surface-breaking flaws in thin materials by using oblique incidence shear waves. Finite element simulations of a water immersion tank set-up were developed to model the ultrasonic response of small back surface-breaking cracks in 0.25 in thick Aluminum 6061 samples. The effect of changes in the crack geometry such as crack length, width, tip morphology, and inclination angle on the optimal oblique incidence angle for crack detection was examined. More specifically, crack lengths between 30 μm and 330 μm in increments of 50 μm and inclination angles between 10° and 80° increments of 10° were examined. Finally, various combinations of rounded or flat crack tip morphologies and 10 μm and 20 μm widths were simulated. The optimal oblique incidence angle varied between 38°, 39°, and 40° depending on the crack height and inclination angle while the introduction of different crack tip morphologies and crack widths had little effect. Future work will be completed on 0.125 in thick Aluminum 6061 samples and more intermediate crack lengths to identify the generalizability of findings.

Ultrasonic nondestructive characterization of cold sintered dielectric microstructures at various scales

Christopher Wheatley Jr., Clive A. Randall and Andrea P. Argüelles

The Cold Sintering Process (CSP) is a novel manufacturing process that can create high-density metals, ceramics, and composite materials at significantly lower temperatures than conventional sintering. However, the microstructure of cold sintered materials can be more flawed and inhomogeneous than observed in conventionally sintered counterparts. Therefore, more information about the underlying densification mechanisms is required to reduce these flaws and promote CSP as an alternative industrial process. Ultrasonic testing provides a non-destructive approach to analyzing the microstructure of these cold-sintered materials. In this presentation, longitudinal attenuation and wave speed are used to characterize sodium molybdate (Na2Mo2O7), a dielectric material. The range of measured values for ultrasonic and attenuation values are consistent across four manufactured thicknesses. These results support CSP as a scalable manufacturing technique for electronic ceramics. Further ultrasonic analysis will go into understanding the densification process, which is ultimately dependent on balancing the kinetics of the transient liquid phase as it undergoes pressure-solution precipitation and evaporation. Finally, the processing parameters will be adjusted using information from ultrasonic characterization to optimize for a homogeneous microstructure, showing CSP as a promising lower-energy alternative for sintered materials.

Towards a Multiscale Approach to Model Nonlinear Wave Propagation for Characterization of Metallic Components

Colin Williams, Matthew Lear, and Parisa Shokouhi

Ultrasonic nondestructive evaluation (NDE) has been extensively used for defect detection, materials characterization, and quality assurance of metallic components. Linear ultrasonic parameters such as wave speed and attenuation are suitable for evaluating microstructural features on the order of the incident wavelength, including grain size and porosity, while nonlinear ultrasonic parameters offer heightened sensitivity to micro-scale features, including dislocations, microcracks, and precipitates. For the nonlinear ultrasonic method of Second Harmonic Generation (SHG), existing work has related the relative acoustic nonlinearity parameter to microstructural features and their evolution under fatigue damage, heat treatment, thermal degradation, and other conditions. These relative trends demonstrate the capability of SHG for materials characterization in individual case studies. Because fabricating and evaluating large sample sets with well-characterized microstructures is time and cost-prohibitive, a unified and quantitative connection between specific microstructural features and the measured ultrasonic response has yet to be established. Numerical simulations assist the challenges of experimentation by enabling the creation of vast, synthetic datasets amenable to parametric studies. Results from a recent study on the ultrasonic evaluation of additively manufactured components will serve as the starting point for microstructure-informed wave propagation models using finite element analysis. An approach for quantitative, multiscale modeling of nonlinear wave propagation in heterogeneous media will be proposed, along with early progress, perceived challenges, and a case study about the influence of a single monopole dislocation on the acoustic nonlinearity parameter. Establishing quantitative relationships between microstructural features and the nonlinear acoustic

response in metal components will improve the applicability of ultrasonic NDE in broad applications across industries.

Surface and plate wave propagation control using topology-optimized metasurfaces

Daniel Giraldo Guzman, Mary Frecker, and Parisa Shokouhi

The control of surface and plate wave propagation has potential applications across length scales, such as acoustic/elastic filters and sensors, vibration barriers, or seismic and explosive shields for vulnerable structures or even towns. Currently, the design of these metasurfaces is typically achieved through experimentation and parameter-tuned designs, but no systematic design methodology has been established. A topology optimization-based methodology is developed to compose locally resonant metasurfaces with optimized resonant units by tailoring resonance and antiresonance frequencies. The optimization problem minimizes the difference between antiresonance eigenfrequencies and a target frequency and maximizes the difference between resonance eigenfrequencies and the target frequency. Numerical results are presented for multiple case studies in which an array of topology-optimized resonators, namely metasurface, effectively prevents the propagation of surface and plate waves.

Monolithic three-dimensional (3D) integration of two-dimensional (2D) field effect transistors

Darsith Jayachandran, Rahul Pendurthi, Nicholas Trainor, Ying Han, Joan M. Redwing, Yang Yang, and Saptarshi Das

Three-dimensional (3D) integration is an emerging technology that is revolutionizing the semiconductor industry. On one hand, it enables the packaging of more devices per unit volume, also referred to as “More Moore”, while on the other hand, it empowers multifunctionality, also known as “More than Moore”, both of which are key toward the development of low-cost, energy-efficient, and high-performance smart electronic systems. While silicon-based 3D integrated circuits (ICs) are already commercially available, there is limited effort on 3D integration of emerging nanomaterials such as two-dimensional (2D) materials despite their novel functionalities that may benefit many applications. Here we demonstrate monolithic 3D integration of a large volume (in excess of 600 transistors in each tier) of aggressively scaled field effect transistors (FETs) based on monolayer MoS_2 at low-thermal budget (with processing temperature < 185 °C). We also realize 3D circuits and demonstrate multifunctional capabilities including sensing, memory storage, as well as logic gates in any tier across the 3D stack. We believe that our demonstration will pave the path for more sophisticated, highly dense, and functionally divergent ICs with a larger number of tiers integrated monolithically in the third dimension.

Phase field modeling of dendrite growth and crack propagation in solid electrolytes

Dingchuan Xue, Ruyue Fang, and Sulin Zhang

All-solid-state batteries (ASSBs) offer the potential for high-energy-density batteries, but their application is limited by dendrite growth and fracture of solid electrolytes (SEs). In this study, we developed a multiphysics model to predict the dendrite deposition and damage process of SEs, where electro-chemo-mechanical process is strongly coupled with crack propagation. Our model revealed that different nucleation sites of lithium (Li) dendrite are the results of the concentrated electric field, and geometric morphology is the inducement of the inhomogeneous electric field. We found applied pressure can effectively slow down nucleation rate. Our numerical simulations also shed light that mutually facilitated dendrite growth and crack propagation are common in ASSBs, with crack propagation preceding dendrite growth. Additionally, we observed intergranular and intragranular fracture within the solid electrolytes at the microscale level, with dendrite nucleation sites and fracture toughness playing significant roles in crack extension and damage. Our results suggest that applied pressure and constraints can be used to inhibit dendrite growth and change the path of crack extension, providing a possible approach for improving the performance of ASSBs.

An On-chip True Random Number Generator Based on Atomically Thin Two-dimensional Materials

Dipanjan Sen, Harikrishnan Ravichandran, Akshay Wali, Nicholas Trainor, Joan Redwing, and Saptarshi Das

Information security is a critical requirement for most Internet of Things (IoT) edge devices that thrive on data. While software-based encryption and decryption schemes are powerful, the computational and energy requirements can be limiting for many resource-constrained IoT applications. In contrast, hardware-based security schemes are more compelling for such IoT devices and true random number generators (TRNGs) constitute the basic building blocks for such hardware security. While conventional silicon-based and emerging nanomaterial-based TRNGs have been demonstrated in recent years, most necessitate extensive peripherals, which incur additional and undesired energy and area overhead. Here, we introduce a peripheral-free TRNG based on a cascaded three-stage inverter (TSI) made using monolayer MoS_2 field-effect transistors (FETs). We exploit stochastic charge trapping and de-trapping phenomena at and/or near the MoS_2/dielectric interface as the source of randomness and convert it into random bits using the TSI. The generated bits pass the NIST randomness tests without any post-processing ensuring their true random nature. Furthermore, the secure keys generated utilizing these random bits offer high entropy, near-ideal correlation, uniformity, and necessary hamming distance. The energy expenditure for the TRNG was found to be as frugal as 30pJ/bit. Our experimental demonstration highlights the potential of atomically thin 2D materials in developing low power TRNG.

Reconstructing the Internal Vibration Response of Jet Engines from External Sensors using Elastic Net Regression

Evan Bozek and Parisa Shokouhi

The internal vibration response of an engine is of primary concern for the long-term health and performance of jet engines. However, it is expensive and invasive to outfit engines with numerous internal sensors, so externally placed sensors are desired. In this study, we investigate reconstructing the rotor-synchronous vibration response of internal vibration sensors with data from external sensors using elastic net regression. Elastic net regression is a regularized regression approach that minimizes the difference between the model and the target, as well as the model coefficients themselves, leading to a (relatively) sparse model which contains less predictors than ordinary least-squares regression. We find that, for most internal sensors, it is possible to reconstruct the rotor-synchronous vibration response of internal vibration sensors with data from external sensors, although the external sensor selection may vary for different internal sensors. We also investigate the tradeoff between the number external sensors used to reconstruct the internal vibration response and accuracy. Our findings indicate that reducing the number of external sensors produces a marginally less accurate, but acceptable fit to the internal vibration response. This means that fewer external sensors are required to determine the internal response, thereby lowering the production costs for the engine. Additional data are required to test the elastic net models and ensure that our models are robust under different environmental and loading conditions.

Optimization and implementation of dielectric resonator couplings in MRI applications to increase the transmit signal

Federico Krauch, Michael Lanagan, Thomas Neuberger, and Qing Yang

Magnetic Resonance Imaging (MRI) is a unique non-invasive imaging method that allows us to acquire high resolution images of soft tissue. This includes acquiring images of the brain, heart, liver and more organs in search of irregularities. Before a process is approved for use in humans, preclinical studies are performed, which consist of testing the process on animals. A significant focus of MRI research lies on improving these preclinical studies, which is the aim of this work. Signal to Noise Ratio (SNR) is one of the biggest concerns in MRI, as the signal needs to be significantly stronger than the noise around for the resolution to be high. Higher resolution not only allows us to obtain more details in the image, but it also speeds up the process. With higher SNR, less time is required to acquire the image, which means more subjects can be studied in the same amount of time. For standard imaging in MRI, Radio Frequency (RF) coils are used for signal transmission and acquisition. The coil generates a pulse that excites the sample being studied and then picks up the signal generated by the sample being excited. Dielectric resonators present a unique chance to improve the SNR. Dielectric Resonators have the particular property of storing energy within them due to their high permittivity value. This characteristic also allows them to enhance the magnetic field locally and said effect can be taken advantage of to enhance the strength of the magnetic pulses used in MRI, by coupling resonators to RF coils. A significant increase in the magnetic signal will lead to a significant increase in SNR, therefore increasing the resolution of the image without supplying more power to the system. The goal is to improve MRI imaging for the Penn State preclinical community.

A Piecewise Approach to Solving the Thermal Inverse Problem

Grant Klinger

A piecewise solution to the Inverse problem is explored for a finite plate/slab and a hollow, thick-walled cylinder with axial symmetry undergoing thermal loading at a surface. The surface thermal loading is assumed to take the form of a cubic polynomial with four unknown coefficients, and convection is allowed to occur on the opposite surface where no thermal loading is applied. A Direct solution is defined as a function of time in terms of the cubic polynomial Inverse and Unit response solutions using Duhamel's integral. Response temperature was theoretically constructed at a point on the convective surface of the plate/slab and cylinder at discrete times. The Direct thermal solution was substituted into the cubic spline process to fit the data by finding the four coefficients of the Inverse solution between each set of data points. The Inverse solution is then constructed piecewise on each interval with these four coefficients, allowing for much higher accuracy than that of the Least Squares method. Furthermore, response data that oscillates or abruptly changes slope can easily be modeled by the thermal spline and produces a dependable Inverse solution, whereas the Least Squares method breaks down.

Ultrasonic Evaluation of Cold Sintered ZnO: Investigating Effects of Transient Phase and Heating Rate in Microstructure

Haley Jones, Abdullah Jabr, Clive Randall, Raul Bermejo, Susan Trolier-McKinstry, and Andrea P. Argüelles

The cold sintering process (CSP) enables densification of many ceramics at temperatures below 300°C by utilizing a transient liquid phase in conjunction with uniaxial pressure in an open system. Transient phase chemistry and heating rate have been reported to affect relative density and microstructure, including the shape and distribution of pores, thus affecting mechanical properties. This work uses high frequency ultrasound (20 MHz) to nondestructively characterize the microstructure of cold sintered ZnO of varying relative densities (80-97%) with two different transient phase chemistries: acetic acid (AA ZnO) and formic acid (FA ZnO). The ultrasonic data for samples prepared at various heating rates (1-30°C/min) are compared to microstructural data collected by X-ray Computed Tomography (XCT). Ultrasonic results showed that average longitudinal wave speeds for FA ZnO were approximately 100-200 m/s higher than those of AA ZnO with the standard 10 °C/min heating rate, indicating a higher relative density. Wave speed measurements on FA ZnO prepared with different heating rates revealed significantly improved spatial homogeneity of the densification for low heating rates and degraded microstructures for high heating rates during CSP. Analytical models for wave speed dependence on porosity, based on the Hashin-Shtrikman and Eshelby-Wu models, revealed that oblate pores perpendicular to the applied pressure direction dominated the wave speeds for both sample sets, which was verified by XCT analysis.

Acceleration of Noise-immune Spiking Neural Network using Stochastic Defect Dynamics in Atomically Thin Transistors

Harikrishnan Ravichandran, Shiva Subbulakshmi Radhakrishnan, and Saptarshi Das

Inferring information in the presence of noise is a challenging task even for the most advanced artificial neural networks (ANNs). In contrast, biological brains process information in the presence of noise and successfully execute various tasks. A key difference arises from information encoding; unlike deterministic encoding used by ANNs, biological neural networks dedicate specialized afferent neurons to encode external and internal stimuli into stochastic spike trains, which leads to energy-efficient and noise-immune computation in the brain. Here, we show that the random telegraph signal (RTS) due to a single defect in an atomically thin field effect transistor (FET) can mimic the stochastic spike encoding functionality of afferent neurons. By controlling the relative energetic position of the defect state through gate electrostatics, we are able to control the mean inter-spike interval, which in turn enables rate-based spike encoding. Finally, we show that medical MNIST images encoded into stochastic spike trains can be inferred better in the presence of noise with an accuracy of > 86% using a trained spiking neural network (SNN) when compared to deterministic encoding.

High-Throughput Bioprinting of the Nasal Epithelium using Patient-derived Nasal Epithelial Cells

I. Deniz Derman, Miji Yeo, Diana Cadena Castaneda, Megan Callender, Mian Horvath, Zengshuo Mo, Ruoyun Xiong, Elizabeth Fleming, Phylip Chen, Mark E. Peeples, Karolina Palucka, Julia Oh, and Ibrahim T. Ozbolat

Human nasal epithelial cells (hNECs) are an essential cell source for the reconstruction of the respiratory pseudostratified columnar epithelium composed of multiple cell types in the context of infection studies and disease modeling. Hitherto, manual seeding has been the dominant method for creating nasal epithelial tissue models through biofabrication. However, this approach has limitations in terms of achieving the intricate 3D structure of the natural nasal epithelium. 3D Bioprinting has been utilized to reconstruct various epithelial tissue models, such as cutaneous, intestinal, alveolar, and bronchial epithelium, but there has been no attempt to use of 3D bioprinting technologies for reconstruction of the nasal epithelium. In this study, for the first time, we demonstrate the reconstruction of the nasal epithelium with the use of primary hNECs deposited on Transwell inserts via droplet-based bioprinting (DBB), which enabled high-throughput fabrication of the nasal epithelium in Transwell inserts of 24-well plates. DBB of nasal progenitor cells ranging from one-tenth to one-half of the cell seeding density employed during the conventional cell seeding approach enabled a high degree of differentiation with the presence of cilia and tight-junctions over a 4-week air-liquid interface culture. Single cell RNA sequencing of these cultures identified five major epithelial cells populations, including basal, suprabasal, goblet, club, and ciliated cells. These cultures recapitulated the pseudostratified columnar epithelial architecture present in the native nasal epithelium and were permissive to respiratory virus infection. These results denote the potential of 3D bioprinting for high-throughput fabrication of nasal epithelial tissue models not only for infection studies but also for other purposes such as disease modeling, immunological studies, and drug screening.

Controlling surface waves in granular media at seismic frequencies using a meta-barrier

Lalith Sai Srinivas Pillarisetti, Cliff J. Lissenden and Parisa Shokouhi

Controlling surface wave propagation is essential to protect critical civil infrastructure and urban areas from the disastrous impact of earthquakes and nuclear blasts. Locally resonant metamaterials offer an unconventional approach to suppress surface waves by generating frequency bandgaps owing to their unnatural material properties attained from the hybridization of the incident wave with the local resonances of the surface-embedded resonators. Particularly, surface waves in homogenous elastic half-space, called Rayleigh waves, predominantly delocalize into shear waves that propagate into the half-space within these bandgap frequencies. However, materials systems of interest for seismic meta-barriers are heterogenous with a power-law dependence of the elastic properties with the depth. Considerations of the material inhomogeneity result in infinite dispersive surface wave solutions called guided surface acoustic modes (PSV and SH modes) and prevent the surface wave delocalization at the bandgap frequencies. A clear understanding of the hybridization between the surface modes in granular media and the local resonances of the resonators is not well established despite being critical in designing realistic and efficient meta-barriers for surface wave suppression. In this work, for the first time, we propose a meta-barrier comprising partially embedded prismatic rod-like resonators to suppress the fundamental surface wave modes in granular media (PSV1 and PSV2) in the seismic frequency range (1 - 30 Hz). The dispersion analysis of the periodic arrangement of resonators and extensive frequency-domain finite element analyses reveal critical hybridizations of the PSV1 and PSV2 modes with longitudinal and flexural resonances that can be exploited for surface wave suppression. We also demonstrate innovative meta-barrier configurations based on an optimal choice of resonator spacing and using geometrically graded resonators for enhanced suppression of the PSV1 and PSV2 modes. With further parametric tuning of the resonant unit-cell geometry, this meta-barrier can find applications in vibration mitigation and seismic isolation of structures.

A ray tracing approach to focusing ultrasonic beams in isotropic and anisotropic solids

Lauren Katch and Andrea P. Argüelles

Focal depths in solid materials are generally calculated using analytical expressions that rely on the paraxial approximation (i.e., small angles related to shallow focusing). However, with increasing use of highly focused probes for acoustic microscopy and backscattering studies, these assumptions are often challenged. Additional challenges are posed by the presence of material anisotropy within the solid. In this presentation, we present a ray tracing-based approach to characterize ultrasonic beam focusing when using highly focused ultrasonic transducers. The results are compared to traditional methods to calculate focal regions to evaluate the range of applicability for isotropic and anisotropic materials. For isotropic solids, a non-paraxial focusing equation is derived and compared to the conventional focusing equation for both normal incidence and oblique incidence immersion setups. Both focusing equations are compared through ray diagrams where the proximity to the true geometric focus is explored. The proposed focusing equation results in a closer approximation to the geometric focus, a smaller beam cross-section, and a greater time convergence compared to the conventional focusing equation. Lastly, the results are expanded to anisotropic media where potential for multiple foci and complex beam behavior arise.

High-speed synchrotron x-ray imaging of micro-scale cavitation in laser-generated molten melt pools

Lovejoy Mutswatiwa, Lauren E. Katch, Andrea P. Argüelles, Nathan Kizer, Tao Sun, Samuel J. Clark, Jordan S. Lum, David M. Stobbe, and Christopher M. Kube

Cavitation phenomena in liquids have been proven helpful in liquid metal processing, wastewater treatment, cleaning, and biomedical applications. In liquid metal processing, cavitation is an alternative to chemical and thermal treatment processes for degassing, inclusion de-agglomeration, grain refinement, and mechanical property enhancement. Significant progress has been made in characterizing macro-scale cavitation in low-temperature and transparent liquids. However, only some studies have attempted to explore micro-scale cavitation in high-temperature fluids such as molten metals. Challenges encountered in micro-scale cavitation studies in opaque liquids include difficulty in sample handling and bubble visualization. Furthermore, in most cavitation studies, a liquid sample of interest already exists, where tension or energy deposition-based techniques break the molecular liquid bonds resulting in phase transformation and cyclic bubble formation-growth and collapse. In some cases, solid phases may need to be melted and induce cavitation simultaneously, presenting a new challenge of high spatial and temporal resolution in observing micro-scale cavitation. This scenario is common in additive manufacturing, where a heat source melts solid powdered particles, typically a laser. At the same time, attempts to leverage cavitation for grain refinement and mechanical property enhancement are made. Here we present a technique capable of directly observing cavitation bubbles in a laser-generated melt pool on an Al6061 sample. A high-energy ultrafast Synchrotron X-ray imaging technique available at the Advanced Photon Source at Argonne National Laboratory was utilized in this study.

An Atomically Thin, Ferromagnetic, Photosensitive, and Programmable Vanadium Disulfide Memtransistor

Mayukh Das, Akshay Wali, Amit Kumar Patel, Suyansh Rai, Amit K. Puthirat, Pulickel M Ajayan, Anchal Srivastava, and Saptarshi Das

Intrinsically ferromagnetic and semiconducting two-dimensional (2D) H-phase vanadium disulfide (VS_2) is promising for future electronics, optoelectronics, spintronics, and valleytronics applications. However, its thermodynamic instability and the formation of intermediate stoichiometric polymorphs during its growth have stymied the progress toward the synthesis of high-quality monolayer VS_2 films. In this article, we circumvent these challenges and accomplish large-area growth of monolayer VS_2 films using the atmospheric pressure chemical vapor deposition (APCVD) technique. By incorporating excess sulfur during the growth process which suppresses the formation of intermediate compounds, good quality large-area monolayer VS_2 film was synthesized. Besides high-resolution atomistic imaging, and Raman and photoluminescence spectroscopy, room-temperature ferromagnetism was experimentally demonstrated in the monolayer film using magnetic force microscopy. Additionally, the electronic and optoelectronic properties of VS_2 were explored by fabricating three-terminal memtransistor devices, which reveal unipolar n-type carrier transport along with a high responsivity to visible light. Finally, non-volatile, and analog programmability of VS_2 memtransistors was demonstrated. To the best of our knowledge, this is the first comprehensive report on the multifunctional capability of any large area-grown 2D monolayer that includes ferromagnetism, photosensitivity, n-type unipolar carrier transport, and non-volatile programmability.

3D Embedded Printing of Microfluidic Devices using a Functional Silicone Composite Support Bath

Mecit Altan Alioglu, Yogendra Pratap Singh, Momoka Nagamine, Syed Hasan Askari Rizvi , Vaibhav Pal , Ethan Michael Gerhard, Shweta Saini , Myoung Hwan Kim, and Ibrahim T. Ozbolat

Over the last two decades, microfluidic devices have rapidly emerged as revolutionary platforms for research and medicine. Various kinds of materials and fabrication strategies have been used to manufacture microfluidic devices; however, most of these strategies face challenges including complexity, time consumption, and cost in recreating delicate and intricate structural organizations. Herein, a silicone composite (Si-Co) was developed and employed as a functional support bath in which a sacrificial ink was 3D printed using embedded printing, enabling freeform fabrication of complex-shaped microfluidic devices. Si-Co was a soft material that had high optical transparency and tunable mechanical properties and yield stress with self-recovering ability. Sacrificial ink filaments formed inside the Si-Co support bath were found to be stable and circular with a wide range of resolution reaching up to 50 μm in channel size. The strategy was exemplified by fabricating microfluidic devices for generation of stable microgels of various sizes. To confirm biocompatibility of Si-Co, induced-pluripotent stem cell-derived endothelial cells were lined up inside microfluidic channels to obtain vascular mimics. Additionally, proof-of-concept spheroid fabrication devices were generated. Overall, the presented strategy allows for facile, rapid, cost-effective, and high-resolution printing and presents potential for the development of microfluidic devices for various applications.

Porosity quantification of metallic components based on synthetic ultrasonic signals using Deep Learning

Michail Skiadopoulos and Parisa Shokouhi

Additively manufactured metallic components may contain subsurface porosity due to errors in their processing parameters. Pores may act as crack initiation sources and lead to failure, so their efficient characterization is essential. Ultrasonic testing (UT) has been widely used in these applications, by propagating a pulse in the defective sample and characterizing it based on extracted features (wave speed, attenuation, etc.) of the received signal. Even though, many analytical scattering models associate these features with the total porosity and the pore size distribution, the simplifying assumptions involved in terms of pore size and shape prevent them from accurately retrieving the pore structure. Therefore, many researchers implement Machine Learning (ML) in the ultrasonic signals to quantify the pore size distribution. We propose the implementation of a Neural Network (NN) model to predict the number of pores and the average pore size from the simulated ultrasonic response of aluminum components containing randomly distributed voids. For this purpose, using ABAQUS along with Python coding, 2D Finite Element (FE) models simulating the pulse-echo testing are developed. The number of voids is varied in the range 3 – 33, the average void radius is varied in the range 25 – 100 μm and the standard deviation of void radius in the range 0 – 25 μm. For each combination of the parameters, 2 realizations were created to account for different positioning of voids, which provided in total 2003 signals. Finally, a feed forward NN model, used as a multi-tasking repressor, is trained, validated and tested solely on the artificial dataset and makes predictions on the number of pores and average pore size. It is observed that while the performance on the prediction of the number of pores is accurate (R2 =

0.81), the model fails to generalize when predicting the average pore radius and further study is needed.

In-situ Transmission electron microscopy to unravel complex corrosion mechanisms

Muhammad Jahangir Khan Lodhi, Ying Han, Zhiyu Zhang, E. Sikora, and Yang Yang

Corrosion is one of the most prevalent forms of material degradation under aggressive environments. Understanding localized corrosion phenomenon at an early stage is pivotal for gaining insight into corrosion mechanisms and developing strategies to mitigate corrosion-caused failures. Despite numerous research efforts for several decades, the mechanisms of corrosion degradation at the nanoscopic scale are still not well understood. Studying the corrosion initiation events at a nanoscopic scale requires state-of-the-art analytical technique with an adequate spatial and temporal resolution simultaneously. In-situ Transmission electron microscopy (TEM) is found to be an extremely insightful approach for unrevealing physical and chemical dynamic processes at small length- and time- scales to provide comprehensive understanding on the origin of corrosion. In contrast to conventionally used, in-situ TEM allows for real-time monitoring of morphological, structural, and compositional evolutions in materials during corrosion phenomenon. In this talk, we will share our recent study of the early-stage oxidation in nickel-based medium entropy alloy (MEA) system at elevated temperatures and under varying environmental conditions using in-situ TEM techniques. The limitations and challenges of such experiments will also be discussed.

A Bio-inspired Visuotactile Neuron for Multisensory Integration

Muhtasim Ul Karim Sadaf, Najam U Sakib, Andrew Pannone, Harikrishnan Ravichandran, and Saptarshi Das

Multisensory integration is a salient feature of the brain, which enables better and faster response in comparison to unisensory integration especially when the unisensory cues are weak. Specialized neurons that receive convergent input from two or more sensory modalities are responsible for such multisensory integration. Solid-state devices that can emulate the response of such multisensory neurons can advance neuromorphic computing and bridge the gap between artificial and natural intelligence. Here we introduce an artificial visuotactile neuron based on the integration of photosensitive monolayer MoS2 memtransistor and a triboelectric tactile sensor, which minutely capture the three essential features of multisensory integration, namely, “super-additive” response, “inverse effectiveness effect”, and “temporal congruency”. We also realized a circuit, which can encode visuotactile information into digital spiking events, with the probability of spiking determined by the strength of the visual and tactile cues. We believe that our comprehensive demonstration of bio-inspired and multisensory visuotactile neuron and spike encoding circuitry will advance the field of neuromorphic computing, which has primarily focused on unisensory intelligence and information processing.

Temperature Mapping for Superconducting Radio-Frequency Cavities Using Type-II Fiber Bragg Grating Sensors

Nailah Oliver, Fatimatou Ndao, Mattia Checchin, Justin Schwartz, Derek Rountree, and Federico Scurti

Superconducting radiofrequency (SRF) cavities are a key component of particle accelerators for high energy physics research, medical and materials applications. The ability to monitor the temperature of the cavity as a function of position allows for enhancing cavity design and performance limits. Type-II fiber Bragg grating (FBG) sensors fabricated by femtosecond-laser inscription are used to map the temperature on a niobium SRF cavity. One significant advantage of type-II sensors over type-I sensors is their immunity to Bragg wavelength alteration caused by changes in the refractive index of silica when exposed to high radiation environments, such as in a SRF cavity. Thus, this radiation immunity was exploited and the attachment of the sensors onto the cavity was refined to promptly monitor the temperature of the cavity. This work demonstrates the ability to detect temperature changes in the <20 K temperature range using the type-II FBG sensors as a direct application for temperature mapping of SRF cavities. An additional benefit of using fiber optic sensors lies in the ability to add a pressure sensor based on Extrinsic Fabry-Perot Interferometry (EFPI) on the same optical fiber that houses the series of type-II FBGs, leading to a simultaneous temperature and pressure measurement and a reduction of cables and feedthroughs penetrating the cryomodule.

Ultra-scaled Contacts to Monolayer MoS_2 Field Effect Transistors

Najam Sakib, Thomas Schranghamer, Muhtasim Ul Karim Sadaf, Shiva Subbulakshmi Radhakrishnan, Rahul Pendurthi, and Saptarshi Das

Contacts to atomically thin two-dimensional (2D) semiconductors remain an open field for research. While achieving low contact resistance ($\boldsymbol{R_C}$) is critical, contact scalability, reproducibility, and manufacturing process compatibility are equally important for any contact engineering strategy to be ultimately successful and industrially applicable. This is more so because contact scaling leads to an increase in $\boldsymbol{R_C}$. Yet, without a scaled contact one cannot claim to have achieved scaled devices with high performance. Here, we investigate Bi, Ni, and Au contacts to monolayer MoS_2 field effect transistors (FETs) with channel lengths ($\boldsymbol{L_{CH}}$) down to 100 nm and found that Au contacts outperform Bi and Ni contacts for a contact length ($\boldsymbol{L_C}$) of 300 nm. Au contacts are then scaled down to $\boldsymbol{L_C}$ = 20 nm to evaluate the impact of contact scaling on the FET performance. Interestingly, Au contacts are found to be relatively immune to scaling with ~ 2.5× reduction in the ON-current, from 519 µA/µm to 206 µA/µm, when L_C is scaled from 300 nm to 20 nm. A high ON-current of 590 µA/µm was achieved for an MoS_2 FET with $\boldsymbol{L_{CH}}$ and $\boldsymbol{L_C}$ both equal to 100 nm. At the same time, the relatively high melting point of Au eliminates processing challenges. As 2D materials enter a new phase of scrutiny for imminent industrial/commercial implementation, it is our belief that this study is warranted to ensure accurate representation of contact effects at the relevant technology nodes currently occupied by silicon.

General Solution for a Single-Phase Conduction Problem of a Finite-Slab with a Growing or Receding Boundary

Pavan Kumar, Albert Segall, and Corina Drapaca

Thermal conduction considerations of a solid media with moving boundaries are of great interest in many research areas. Unfortunately, it is very difficult to find analytical or semi-analytical solutions for the single-phase heat equation in real time with a growing or receding boundary. While non-numerical solutions for infinite and semi-infinite domains are available, these cannot accurately model many common situations. In order to overcome this shortcoming, a semi-analytical solution for the heat equation for a single phase, homogeneous, and finite-slab with a growing or receding boundary under unit loading was derived in the Laplace domain and a series representation then was used to approximate the inverse Laplace transform in the time domain. Predictions were compared to finite element solutions with good agreement obtained for low to moderate growth or recession rates. Applications of the resulting kernel could include the direct or inverse prediction of temperatures during machining, wear, corrosion, and/or additive manufacturing via cold-spray.

Predicting laboratory-scaled shear failure from time-lapse active source ultrasonic data using a physics-informed neural network (PINN) model

Prabhav Borate, Jacques Rivière, Chris Marone, Ankur Mali, Daniel Kifer, and Parisa Shokouhi

In various fields, including civil, transportation, and geophysics shear failure prediction is crucial. The task of failure prediction though challenging is important for safe operations. Earthquakes, a type of shear failure, occur suddenly and pose a major hazard to humanity. So, preventing such catastrophic events and lowering the loss of lives would have a significant positive social impact. Previous laboratory-scaled friction experiment studies coupled with ultrasonic monitoring have shown that shear failure (shear stress and failure timing) can be predicted using machine learning (ML) and deep learning (DL) models developed using the wave features namely wave speed, wave amplitude, and center frequency. These entirely data-driven models, which require a sizable training dataset, might not generalize very well. In this study, we investigate the implementation of the physics-informed neural network (PINN) approach with the hypothesis that it will reduce the training data size, improve the overall model predictions, and make the models transferable from one experimental dataset to another. The data from the friction experiment coupled with ultrasonic monitoring using a pair of P-wave transducers is used. The wave speed and amplitude extracted from the ultrasonic signals are used as inputs to the model. To implement the physics constraint, we incorporate the equation relating the elastic coupling of fracture with the surrounding medium and fracture stiffness to the ultrasonic transmission coefficient relation. Also, to study the model generalizability the transfer learning (TL) models are developed and compared against the models trained without any previous information. Our results demonstrate that the inclusion of the physics constraints in the DL framework improves the shear failure predictions compared to the data-driven model.

Alteration of Optical Bragg Phenomenon by Substrate Roughness

Ricardo A. Fiallo, Chengzhi Li, Mark W. Horn, and Akhlesh Lakhtakia

A Bragg mirror is a dielectric slab that is periodically nonhomogeneous in the thickness direction. It displays the Bragg phenomenon as a high-reflectance spectral regime that depends on the direction of propagation and the polarization state of the incident light. Implicit in both theoretical treatments and fabrication procedures is the smoothness of the surface on which the Bragg mirror is fabricated. We have found that the Bragg phenomenon exhibited in the visible regime by periodically nonhomogeneous thin films grown on glass substrates can be significantly affected, even nullified, by pre-fabrication roughening of the surface of the substrate.

Gamma Radiation Resilience of Two-Dimensional Electronics based on MoS_2

Thomas Schranghamer, Andrew Pannone, Harikrishnan Ravichandran, Sergei P. Stepanoff, Nicholas Trainor, Joan M. Redwing, Douglas E. Wolfe, and Saptarshi Das

Limitations in cloud-based computing have prompted a paradigm shift towards all-in-one "edge" devices capable of independent data sensing, computing, and storage. Advanced defense and space applications stand to benefit immensely from this due to their need for continual operation in areas where maintaining remote oversight is difficult. However, the extreme environments relevant to these applications necessitate rigorous testing of new technologies, with a common requirement being hardness to ionizing radiation. Two-dimensional (2D) molybdenum disulfide (MoS_2) has been noted to enable the sensing, storage, and logic capabilities necessary for all-in-one edge devices. Despite this, the investigation of ionizing radiation effects in MoS_2-based devices remains incomplete. In particular, studies on gamma radiation effects in MoS_2 have been largely limited to standalone films, with few device investigations; to the best of our knowledge, no explorations have been made into gamma radiation effects on the sensing and memory capabilities of MoS_2-based devices. In this work, we have used a statistical approach to study high-dose (1 Mrad) gamma radiation effects on photosensitive and programmable memtransistors fabricated from large-area monolayer MoS_2. Memtransistors were divided into separate groups to ensure accurate extraction of device characteristics pertaining to baseline performance, sensing, and memory before and after irradiation. All-MoS_2 logic gates were also assessed to determine gamma irradiation impact on logic implementation. Our findings show that the multiple functionalities of MoS_2 memtransistors are not severely impacted by gamma irradiation even without dedicated shielding/mitigation techniques. We believe that these results serve as a foundation for more application-oriented studies going forward.

High-throughput microgel fabrication via air-assisted co-axial jetting for cell encapsulation, 3D bioprinting, and scaffolding applications

Vaibhav Pal, Yogendra Pratap Singh, Deepak Gupta, Mecit Altan Alioglu, Momoka Nagamine, Myoung Hwan Kim, and Ibrahim Tarik Ozbolat

Microgels have recently received widespread attention for their applications in a wide array of domains such as tissue engineering, regenerative medicine, and cell and tissue transplantation because of their properties like injectability, modularity, porosity, and the ability to be customized in terms of size, form, and mechanical properties. However, it is still challenging to mass produce (high-throughput) microgels with diverse sizes and tunable properties. Herein, we developed an

air-assisted co-axial device (ACAD) for continuous production of microgels in a high-throughput manner. To test its robustness, microgels of multiple hydrogels and their combination, including alginate (Alg), gelatin methacrylate (GelMA) and Alg-GelMA, were formed at a maximum production rate of ~65,000 microgels per sec while retaining circularity and a size range of 50-500 µm based on varying air pressure levels. The ACAD platform allowed single and multiple cell encapsulation with 74±6% efficiency. These microgels illustrated appealing rheological properties such as yield stress, viscosity, and shear modulus for bioprinting applications. Specifically, Alg microgels have the potential to be used as a sacrificial support bath while GelMA microgels have potential for direct extrusion both on their own or when loaded in a bulk GelMA hydrogel. Generated microgels showed high cell viability (>90%) and proliferation of MDA-MB-231 and human dermal fibroblasts over seven days in both encapsulation and scaffolding applications, particularly for GelMA microgels. The developed strategy provides a facile and rapid approach without any complex or expensive consumables and accessories for scalable high-throughput microgel production for cell therapy, tissue regeneration and 3D bioprinting applications.

Graphene Strain-effect Transistor with Colossal ON/OFF Current Ratio Enabled by Reversible Nano-crack Formation in Metal Electrodes on Piezoelectric Substrates

Yikai Zheng, Dipanjan Sen, Sarbashis Das, and Saptarshi Das

Extraordinarily high carrier mobility in graphene has led to many remarkable discoveries in physics and at the same time invoked great interest in graphene-based electronic devices and sensors. However, the poor ON/OFF current ratio observed in graphene field-effect transistors has stymied its use in many applications. Here, we introduce a graphene strain-effect transistor (GSET) with a colossal ON/OFF current ratio around 10^7 by exploiting strain-induced reversible nano-crack formation in the source/drain metal contacts with the help of a piezoelectric gate stack. GSETs also exhibit steep switching with a subthreshold swing (SS) < 1 mV/decade averaged over ~ 6 orders of magnitude change in the source-to-drain current for both electron and hole branch amidst a finite hysteresis window. We also demonstrate high device yield and strain endurance for GSETs. We believe that GSETs can significantly expand the application space for graphene-based technologies.

Bandgap Modulation of ZnO Nanowires through Elastic Strain Engineering

Yingxin Zhu and Wang Heyi

ZnO, as a prospective third-generation wide band-gap semiconductor, is highly competitive for future applications in semiconductor optoelectronics due to its intrinsic optoelectronic and mechanical advantages over conventional semiconductors, including high electron mobility and super elastic strain properties. Considering the undesirable effects of phosphors and the irreversible chromaticity shift in existing luminescent materials, we proposed band-gap modulation based on ZnO nanowire over an extensive strain range as the solution, with the advantage of enabling continuous, real-time, and reversible luminescence modulation over a broad range, which promises new insights for semiconductor optoelectronics. To investigate the principle of strain-shift energy band-gap, we modulate the nanowire by mechanical loading/unloading to probe the limits of the elastic strain for an extensive range of color shifts of the luminescence. As the energy band-gap shifts during the tensile test, the nanowires result in a corresponding change in the photons emitted, leading to a variation in color. By applying the "elastic strain engineering" strategy, we achieved the modulation of the semiconductor band-gap from 3.289 eV to 3.229 eV by stretching the nanowire to reach 2.48% strain and explored the correlation. This color shift is continuous, real-time, and reversible, which sheds light on the future development of semiconductor luminescence.

Comprehensive Comparison of the Full-cascade and Quick Calculation Modes in the Monte Carlo Simulation of Ion Irradiation Damage in Monoatomic Targets

Zhiyu Zhang and Yang Yang

Monte Carlo simulations based on the binary collision approximation (BCA) have been widely used to predict the depth profile of primary radiation defects in materials due to ion beam irradiation. The most representative code of those is the Stopping and Range of Ions in Matter (SRIM), where two modes, full-cascade (FC) and quick calculation (QC), are offered in the modeling of primary radiation damage. Confidently utilizing the code to obtain reliable results hinges upon a comprehensive understanding of the difference between FC and QC. However,

because of the low computational efficiency of SRIM, previously only a limited number of cases can be computed to provide insights into this issue. Here, we used IM3D, a SRIM-like code but 1000 times faster, to reveal the discrepancy between FC and QC over the periodic table for four ion energies, including more than 33,586 ion-target combinations. We show that the ratio of vacancy creation by FC/QC based on the direct-output method ranges from 1 to 3, with a fitted normal distribution centered near 1.8 to 2. Surprisingly, this ratio is very weakly dependent on the ion element, suggesting that the intrinsic discrepancy between FC and QC may originate from the different consideration of target effect. By visualizing the results for a selected ion on the periodic table, we further discover that the targets with a high FC/QC ratio appear to be localized at the right half of the transition metal region. Also, we quantitatively unravel the relative error of vacancy depth by QC due to the neglected "forward scattering" effect. The maximum relative error is up to 80% for 1 keV ions, while it decreases rapidly as the ion energy increases. Finally, we show that both the displacement threshold energy and the binding energy can impact the FC/QC ratio significantly. Our results offer the crucial reference for SRIM users to choose between FC and QC, and a quick estimation of the FC vacancy creation in monoatomic targets if the QC result is known.

Poster Presentations

Poster Presentations			
Speaker	**Abstract Title**	**Speaker**	**Abstract Title**
Arnab Chatterjee	*Additive Manufacturing build plan dependence of spatially resolved structure-behavior relations in active materials*	Changhao Li	*Machine Learning Cell Traction Forces*
Christopher Wheatley Jr.	*Ultrasonic nondestructive characterization of cold sintered dielectric microstructures at various scales*	Flor Parra	*Pathological characterization of pediatric postinfectious hydrocephalus*
Irem Deniz Derman	*3D Breathing Lung Model*	Luyi Feng	*Physical forces guide curvature sensing and cell migration mode bifurcating*
Mecit Altan Alioglu	*3D Embedded Printing of Microfluidic Devices using a Functional Silicone Composite Support Bath*	Nathan Kizer	*Online Melt Pool Monitoring for Additive Manufacturing using Ultrasound and Synchrotron X-rays*
Rahul Pendurthi	*Monolithic three-dimensional (3D) integration of two-dimensional (2D) field effect transistors*	Ruyue Fang	*Phase-field modeling of zirconium oxidation induced cracks*
Shiva Subbulakshmi Radhakrishnan	*Ferroelectric field effect transistors with 2D materials as the channel*	Vaibhav Pal	*High-throughput microgel fabrication via air-assisted co-axial jetting for cell encapsulation, 3D bioprinting, and scaffolding applications*
Zhu Yingxin	*Bandgap Modulation of ZnO Nanowires through Elastic Strain Engineering*		

Additive Manufacturing build plan dependence of spatially resolved structure-behavior relations in active materials

Arnab Chatterjee and Reginald Felix Hamilton

Active materials are a new class of material systems that undergo a reversible shape change under external stimuli. Shape Memory Alloys (SMAs) are a class of active materials. In this work, we fabricated Nickel-Titanium based SMAs using Additive Manufacturing (AM). AM is a layer-by-layer manufacturing technique that allows customizing extrinsic size and shape along with intrinsic composition and structure. Laser Directed Energy Deposition (LDED) technique employs pre-blended elemental powder feedstock for controlling SMA composition. As a result of layer/pass wise buildup, the intrinsic factors will vary spatially. Since it is generally accepted that a spatially uniform composition and structure are essential for optimal SMA behavior, varying the AM build plan has been explored in this work for reducing heterogeneity inherent to AM. Two build plans differentiated by the orientation of the tool path with respect to the mechanical loading direction are manufactured. The signatures of layer/pass wise overlapping regions along various build planes have been observed. Microstructural hierarchy and behavior have been spatially investigated along these signatures in locations corresponding to build parameters. Along different planes, the grain morphology varies between equiaxed grains with higher aspect ratio and elongated grains with low aspect ratio. The build plan having higher number of layers have predominant eutectic morphology of second phase along its plane, whereas one having higher number of passes have varying morphologies. The microhardness increases along build direction and along the laser scan direction, it falls from near free edge to the center of the builds. Thus, combined study of X-Ray Diffraction, microscopy, and microhardness can successfully produce spatial maps to demonstrate a local structure-behavior relations to assess impact of AM build plans.

Machine Learning Cell Traction Forces

Changhao Li, Luyi Feng, and Sulin Zhang

Cellular force signaling across a hierarchy of molecular switchers is central to various mechanobiological processes. However, current force microscopies for measuring cellular forces suffer from low throughput and matrix-stiffness dependent low resolution. Here we demonstrate that a generative adversarial network (GAN), trained by hybrid experimental and numerical datasets, can paint out traction force maps of cells. GAN analyzes traction force maps as an image-to-image translation problem, in which its generator and discriminator neural networks can be simultaneously cross-trained. The trained GAN can predict the colony-size and substrate-stiffness dependent traction force maps, with the phase contrast cell images as the only input. For cells on substrates with a stiffness gradient, the GAN predicts asymmetric traction force distribution, which implies durotaxis. Our machine learning model can reveal hidden relationship between substrate stiffness and cell contractility, which is inaccessible to experiments. Without additional training, the machine learning model can be extrapolated to predicting of traction force maps for different cell types with a single scaling factor. The neural network based TFM serves as a high-throughput tool to mapping out the cellular forces in various mechanobiological processes and paves the way toward data-driven discoveries in cell mechanobiology.

Ultrasonic nondestructive characterization of cold sintered dielectric microstructures at various scales

Christopher Wheatley Jr, Clive A. Randall, and Andrea P. Argüelles

The Cold Sintering Process (CSP) is a novel manufacturing process that can create high-density metals, ceramics, and composite materials at significantly lower temperatures than conventional sintering. However, the microstructure of cold sintered materials can be more flawed and inhomogeneous than observed in conventionally sintered counterparts. Therefore, more information about the underlying densification mechanisms is required to reduce these flaws and promote CSP as an alternative industrial process. Ultrasonic testing provides a non-destructive approach to analyzing the microstructure of these cold-sintered materials. In this presentation, longitudinal attenuation and wave speed are used to characterize sodium molybdate (Na2Mo2O7), a dielectric material. The range of measured values for ultrasonic and attenuation values are consistent across four manufactured thicknesses. These results support CSP as a scalable manufacturing technique for electronic ceramics. Further ultrasonic analysis will go into understanding the densification process, which is ultimately dependent on balancing the kinetics of the transient liquid phase as it undergoes pressure-solution precipitation and evaporation. Finally, the processing parameters will be adjusted using information from ultrasonic characterization to optimize for a homogeneous microstructure, showing CSP as a promising lower-energy alternative for sintered materials.

Pathological characterization of pediatric postinfectious hydrocephalus

Flor Parra, Mallory Peterson, Paddy Ssentongo, and Steven Schiff

"Intracranial calcifications (IC’s) are abnormal mineral depositions in the brain parenchyma, commonly associated with a wide range of neurological, metabolic and genetic conditions, as well as acquired viral and bacterial infections. In the present study, computed tomography scans of 135 cases of pediatric hydrocephalus, some with a positive diagnosis of a bacterial infection (Paenibacillus thyaminolyticus), were processed using a customized CT image segmentation tool. Volumetric estimates of clinically identified IC’s, brain tissue, and cerebrospinal fluid were obtained and compared at pre- and post-treatment time points with a three-fold purpose: 1) To characterize the temporal evolution of IC’s in association with a bacterial infection and assess their validity as a biomarker of infection-related neural damage, 2) to investigate the extent of the detriment of the postinfectious hydrocephalus (PIH) in the intracranial vault compared to its non-infectious counterpart (NPIH) 3) Identify other key explanatory variables of infectious process.
It is shown that while the presence of calcifications is a statistically significant biomarker of infection, the relative temporal progression has no association with disease progression. The volumetric estimate of cerebrospinal fluid was identified as the leading classifier of infection.
Given that PIH following neonatal sepsis continues to be the leading cause of pediatric hydrocephalus globally, and the surgically invasive, high-risk nature of the existing treatments, there is a pressing need to improve the characterization of the pathogens that give rise to PIH. This body of work constitutes part of such effort.

3D Breathing Lung Model

I. Deniz Derman, Mecit Altan Alioglu, Momoka Nagamine, Hasan Rizvi, and Ibrahim Tarik Ozbolat

We have created a sophisticated three-dimensional (3D) lung model that is made up of an alveolar epithelial compartment encircled by a vascular compartment with endothelium. The model is designed to facilitate air ventilation and perfusion, and it is printed on a biocompatible plastic platform device using a commercial 3D bioprinter. The device was seeded with Zs Green A549 lung carcinoma cells in the alveolar chamber. A549 cells were subjected to air-liquid culture with air ventilation for a total of 7 days, and the cells were differentiated at the air-liquid interface. The histology of the cells grown was characterized using ZO1 antibody staining. The 7-day old air-liquid interface was then subjected to RFP labeled H1N1 viral infection and allowed to infect.

Overall, 3D breathing lung models offer a valuable tool for studying lung physiology and disease, drug discovery and development, and personalized medicine. As such, they have the potential to significantly improve our understanding of lung biology and improve patient outcomes. For this specific aim demonstrates significant improvements in the design and development of a 3D lung model. The model's biocompatible plastic platform device allows for the perfusion of media and air ventilation, facilitating the growth of endothelial and epithelial cells. The addition of ventilation resulted in the differentiation of A549 cells at the air-liquid interface and increased TEER, demonstrating the model's potential use in studying lung function and disease.

Physical forces guide curvature sensing and cell migration mode bifurcating

Luyi Feng, Changhao Li, and Sulin Zhang

The ability of cells to sense and adapt to curvy topographical features has been implicated in organ morphogenesis, tissue repair, and tumor metastasis. However, how individual cells or multicellular assemblies sense and differentiate curvatures remains elusive. Here we reveal a novel curvature-sensing mechanism in which surface tension can selectively activate either actin or integrin flows, leading to bifurcating cell migration modes: focal adhesion formation that enables cell crawling at convex front edges and actin cable assembly that pulls cells forward at concave front edges. The molecular flows and curved-front morphogenesis are sustained by coordinated cellular tension generation and transmission. We track the molecular flows and mechanical force transduction pathways by a phase field model and predict that multicellular curvature sensing is more efficient than individual cells, suggesting collective intelligence of cells. The unique ability of cells in curvature sensing and migration mode bifurcating may offer insights into emergent collective patterns and functions of living active systems at different length scales.

3D Embedded Printing of Microfluidic Devices using a Functional Silicone Composite Support Bath

Mecit Altan Alioglu, Yogendra Pratap Singh, Momoka Nagamine, Syed Hasan Askari Rizvi, Vaibhav Pal, Ethan Michael Gerhard, Shweta Saini, Myoung Hwan Kim, and Ibrahim T. Ozbolat

Over the last two decades, microfluidic devices have rapidly emerged as revolutionary platforms for research and medicine. Various kinds of materials and fabrication strategies have been used to manufacture microfluidic devices; however, most of these strategies face challenges including complexity, time consumption, and cost in recreating delicate and intricate structural organizations. Herein, a silicone composite (Si-Co) was developed and employed as a functional support bath in which a sacrificial ink was 3D printed using embedded printing, enabling freeform fabrication of complex-shaped microfluidic devices. Si-Co was a soft material that had high optical transparency and tunable mechanical properties and yield stress with self-recovering ability. Sacrificial ink filaments formed inside the Si-Co support bath were found to be stable and circular with a wide range of resolution reaching up to 50 μm in channel size. The strategy was exemplified by fabricating microfluidic devices for generation of stable microgels of various sizes. To confirm biocompatibility of Si-Co, induced-pluripotent stem cell-derived endothelial cells were lined up inside microfluidic channels to obtain vascular mimics. Additionally, proof-of-concept spheroid fabrication devices were generated. Overall, the presented strategy allows for facile, rapid, cost-effective, and high-resolution printing and presents potential for the development of microfluidic devices for various applications.

Online Melt Pool Monitoring for Additive Manufacturing using Ultrasound and Synchrotron X-rays

Nathan Kizer, Lauren Katch, Lovejoy Mutswatiwa, Tao Sun, Samuel J. Clark, Jordan S. Lum, David M. Stobbe, and Christopher M. Kube

Metal additive manufacturing (AM) has been a topic of interest due to its wide versatility in part geometry, material selection, and low-waste production. Many AM processes utilize a high-intensity laser to weld metal powder feedstock to form the desired part geometry. However, poor part quality is throttling the expansion of metal AM. Defects, such as gas porosity caused keyholing, significantly reduce the serviceability of parts produced through AM. A fundamental understanding of how the melt pool geometry and dynamic behavior during fusion and solidification are paramount to creating low-defect welds. The traditional method to monitor melt pools is X-ray imaging conducted using a synchrotron. However, access to a synchrotron is limited and costly and only provides a 2D representation of the melt pools. Immersion ultrasonic inspection has been proposed as a low-cost method to monitor melt pools and provide volumetric measurements. This work utilizes high-speed X-ray imaging to establish a ground truth of the melt pool characteristics and then maps the features to the ultrasonic data collected during the melt pool formation and solidification.

Monolithic three-dimensional (3D) integration of two-dimensional (2D) field effect transistors

Rahul Pendurthi, Darsith Jayachandran, Nicholas Trainor, Ying Han, Joan M. Redwing, Yang Yang and Saptarshi Das

Three-dimensional (3D) integration is an emerging technology that is revolutionizing the semiconductor industry. On one hand, it enables the packaging of more devices per unit volume, also referred to as "More Moore", while on the other hand, it empowers multifunctionality, also known as "More than Moore", both of which are key toward the development of low-cost, energy-efficient, and high-performance smart electronic systems. While silicon-based 3D integrated circuits (ICs) are already commercially available, there is limited effort on 3D integration of emerging nanomaterials such as two-dimensional (2D) materials despite their novel functionalities that may benefit many applications. Here we demonstrate monolithic 3D integration of a large volume (in excess of 600 transistors in each tier) of aggressively scaled field effect transistors (FETs) based on monolayer MoS2 at low-thermal budget (with processing temperature < 185 °C). We also realize 3D circuits and demonstrate multifunctional capabilities including sensing, memory storage, as well as logic gates in any tier across the 3D stack. We believe that our demonstration will pave the path for more sophisticated, highly dense, and functionally divergent ICs with a larger number of tiers integrated monolithically in the third dimension.

Phase-field modeling of zirconium oxidation induced cracks

Ruyue Fang, Dingchuan Xue, Yanzhou Ji, Yang Yang, Long-Qing Chen, and Sulin Zhang

Despite the widespread application of zirconium alloys in nuclear engineering, oxidation may cause cracks and limit their performance. Developing a numerical framework to track the processes of oxidation and fracture could help explain the phenomena and inhibit the corrosion of zirconium alloys. Among the existing numerical models of metal oxidation or cracking, the phase-field model based on diffusive interfaces has the advantage of tracking irregular interfaces. However, a comprehensive model which couples oxidation and cracking has not been reported. Thus, this paper presents a detailed phase-field model to predict the coupled process between zirconium oxidation and crack propagation. The model considers the plastic deformation of the zirconium matrix while the oxide phase is believed to remain pure elasticity. Our results indicate that curvatures may determine the nucleation site of zirconium oxide, which is validated by analytical stress analysis. The oxidation and fracturing are coupled through hydrostatic pressures and first principal stresses, suggesting that the two processes are facilitating each other.

Ferroelectric Field Effect Transistors with 2D Materials as the Channel

Shiva Subbulakshmi Radhakrishnan and Saptarshi Das

An ideal memory system should enable random access, fast speed, low power, high density, and non-volatility. However, the current memory technology relies primarily on the charge trapping in the floating gate structure leading to latency in writing and higher power consumption. Therefore ferroelectric field-effect transistors (FeFET) are considered a strong contender for the next generation of memory technology due to their fast writing speed, reliability, and higher endurance. FeFET consists of a ferroelectric material and a semiconductor on top to perform a non-destructive read operation. Therefore, along with the dielectric, semiconductor also plays an essential role in

realizing an ideal memory device. Since the current technology primarily relies on silicon, where the interface traps are predominant, which may balance out the polarization charge from the ferroelectric material, making it predominantly charge trapping. Therefore, to overcome the interface traps, most semiconductors require a thin buffer oxide layer where the charge trapping gets minimized. However, the thin buffer oxide requires additional voltage to switch the polarization charge making it energy inefficient. Therefore, this research used two-dimensional materials for their inert surface, making them ideal for realizing energy-efficient FeFET.

High-throughput microgel fabrication via air-assisted co-axial jetting for cell encapsulation, 3D bioprinting, and scaffolding applications

Vaibhav Pal, Yogendra Pratap Singh, Deepak Gupta, Mecit Altan Alioglu, Momoka Nagamine, Myoung Hwan Kim, and Ibrahim Tarik Ozbolat

Microgels have recently received widespread attention for their applications in a wide array of domains such as tissue engineering, regenerative medicine, and cell and tissue transplantation because of their properties like injectability, modularity, porosity, and the ability to be customized in terms of size, form, and mechanical properties. However, it is still challenging to mass produce (high-throughput) microgels with diverse sizes and tunable properties. Herein, we developed an air-assisted co-axial device (ACAD) for continuous production of microgels in a high-throughput manner. To test its robustness, microgels of multiple hydrogels and their combination, including alginate (Alg), gelatin methacrylate (GelMA) and Alg-GelMA, were formed at a maximum production rate of ~65,000 microgels per sec while retaining circularity and a size range of 50-500 µm based on varying air pressure levels. The ACAD platform allowed single and multiple cell encapsulation with 74±6% efficiency. These microgels illustrated appealing rheological properties such as yield stress, viscosity, and shear modulus for bioprinting applications. Specifically, Alg microgels have the potential to be used as a sacrificial support bath while GelMA microgels have potential for direct extrusion both on their own or when loaded in a bulk GelMA hydrogel. Generated microgels showed high cell viability (>90%) and proliferation of MDA-MB-231 and human dermal fibroblasts over seven days in both encapsulation and scaffolding applications, particularly for GelMA microgels. The developed strategy provides a facile and rapid approach without any complex or expensive consumables and accessories for scalable high-throughput microgel production for cell therapy, tissue regeneration and 3D bioprinting applications.

Bandgap Modulation of ZnO Nanowires through Elastic Strain Engineering

Yingxin Zhu and Wang Heyi

ZnO, as a prospective third-generation wide band-gap semiconductor, is highly competitive for future applications in semiconductor optoelectronics due to its intrinsic optoelectronic and mechanical advantages over conventional semiconductors, including high electron mobility and super elastic strain properties. Considering the undesirable effects of phosphors and the irreversible chromaticity shift in existing luminescent materials, we proposed band-gap modulation based on ZnO nanowire over an extensive strain range as the solution, with the advantage of enabling continuous, real-time, and reversible luminescence modulation over a broad range, which promises new insights for semiconductor optoelectronics. To investigate the principle of strain-shift energy band-gap, we modulate the nanowire by mechanical loading/unloading to probe the limits of the elastic strain for an extensive range of color shifts of the luminescence. As the energy band-gap

shifts during the tensile test, the nanowires result in a corresponding change in the photons emitted, leading to a variation in color. By applying the "elastic strain engineering" strategy, we achieved the modulation of the semiconductor band-gap from 3.289 eV to 3.229 eV by stretching the nanowire to reach 2.48% strain and explored the correlation. This color shift is continuous, real-time, and reversible, which sheds light on the future development of semiconductor luminescence.

Art in Science

Momoka Nagamine

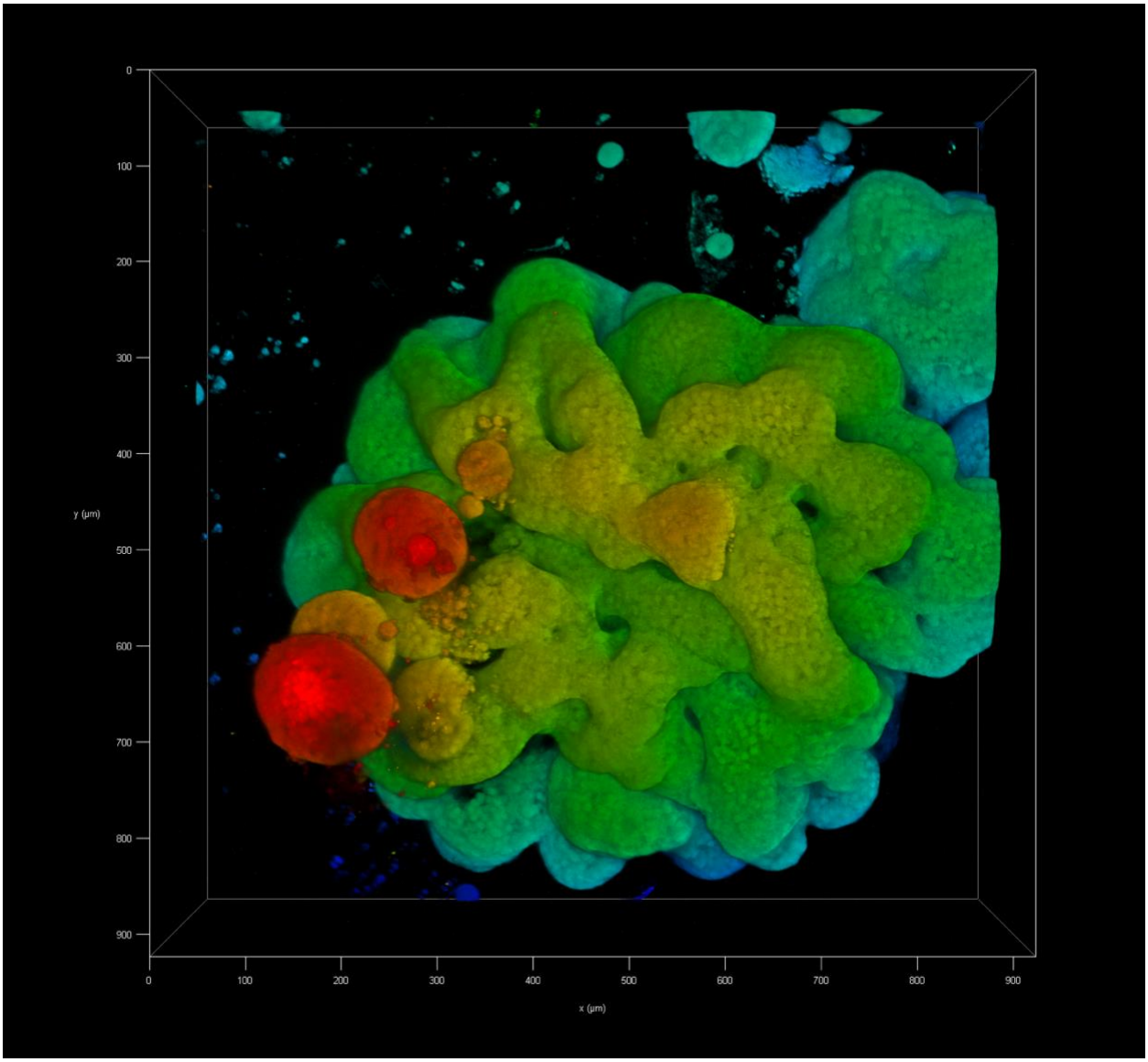

Mecit Altan Alioglu

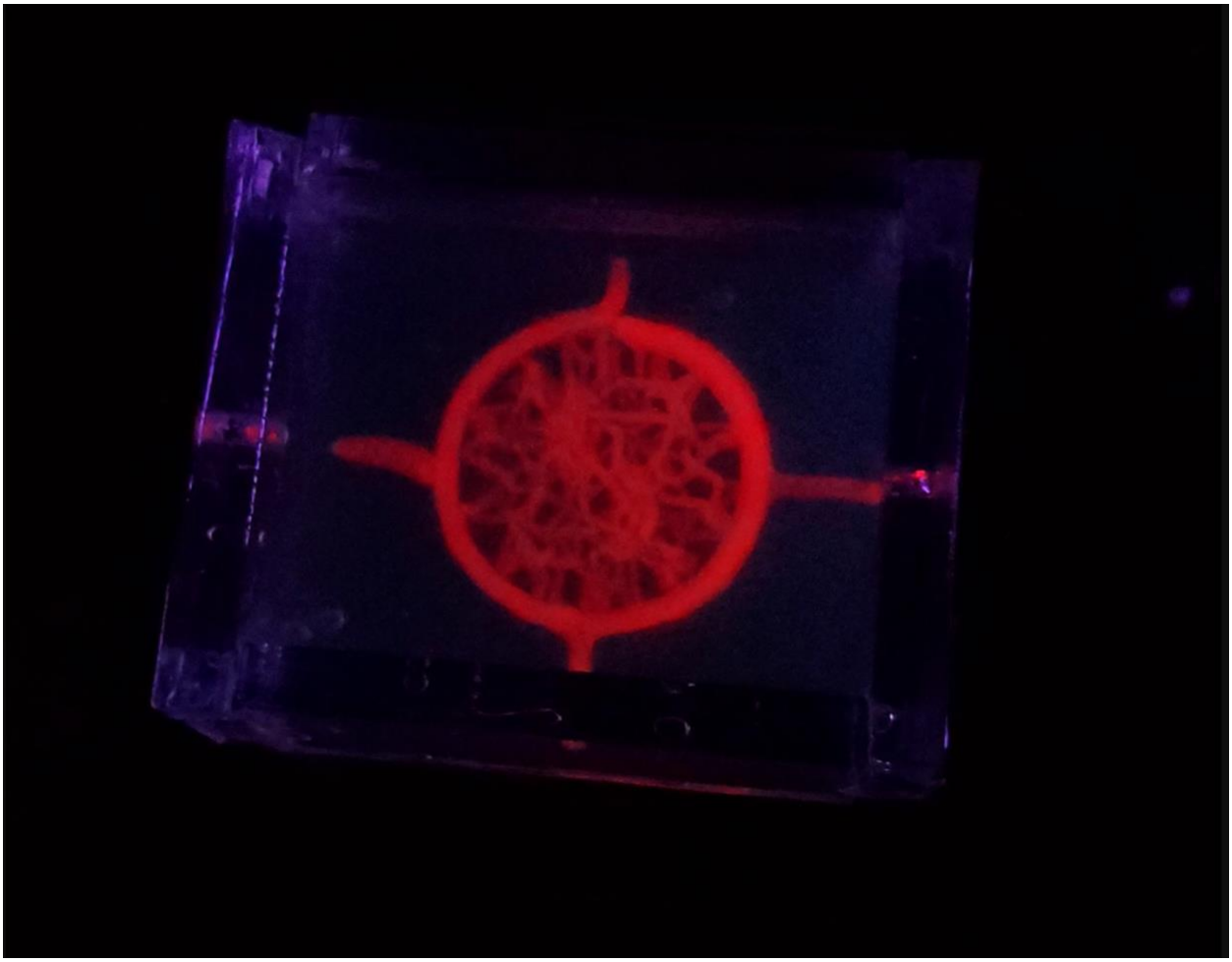

Mayukh Das

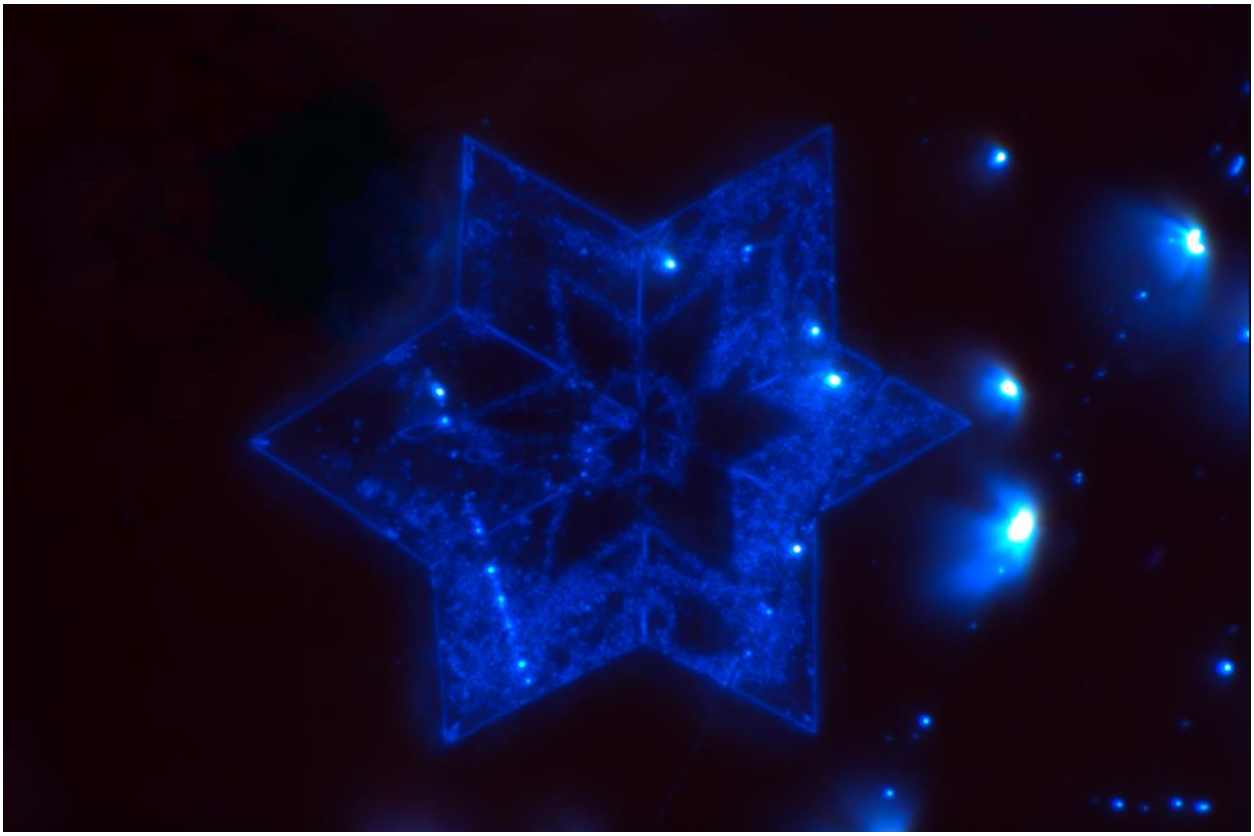

“Micron sized Marbles: Alginate hydrogel microspheres”

Vaibhav Pal

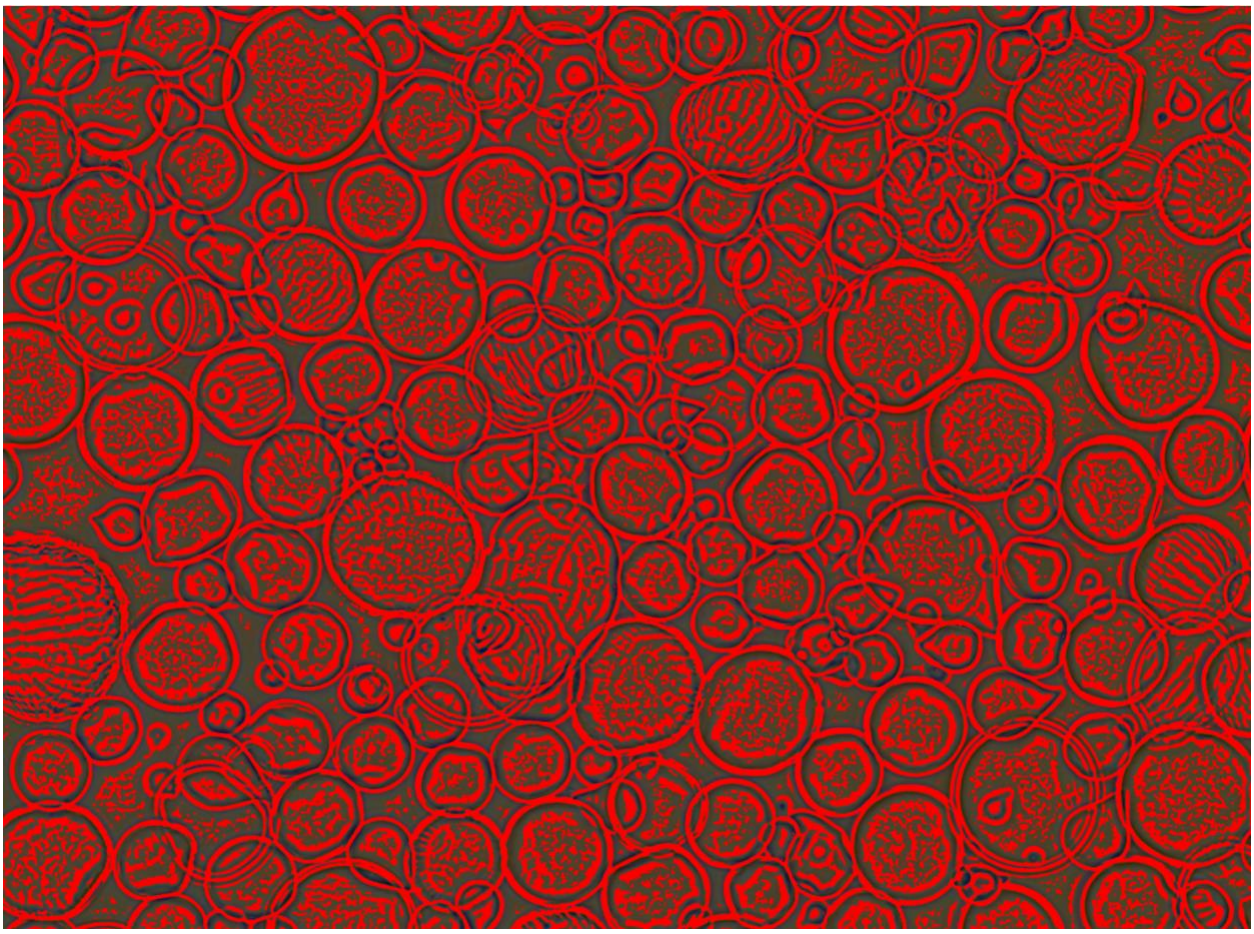

An ImageJ software gure of Alginate microgels generated using a newly developed air-assisted co-axial device (ACAD). These microgels have various potential applications such as encapsulation and delivery of cells and fabricating cell-laden structures via 3D bioprinting.

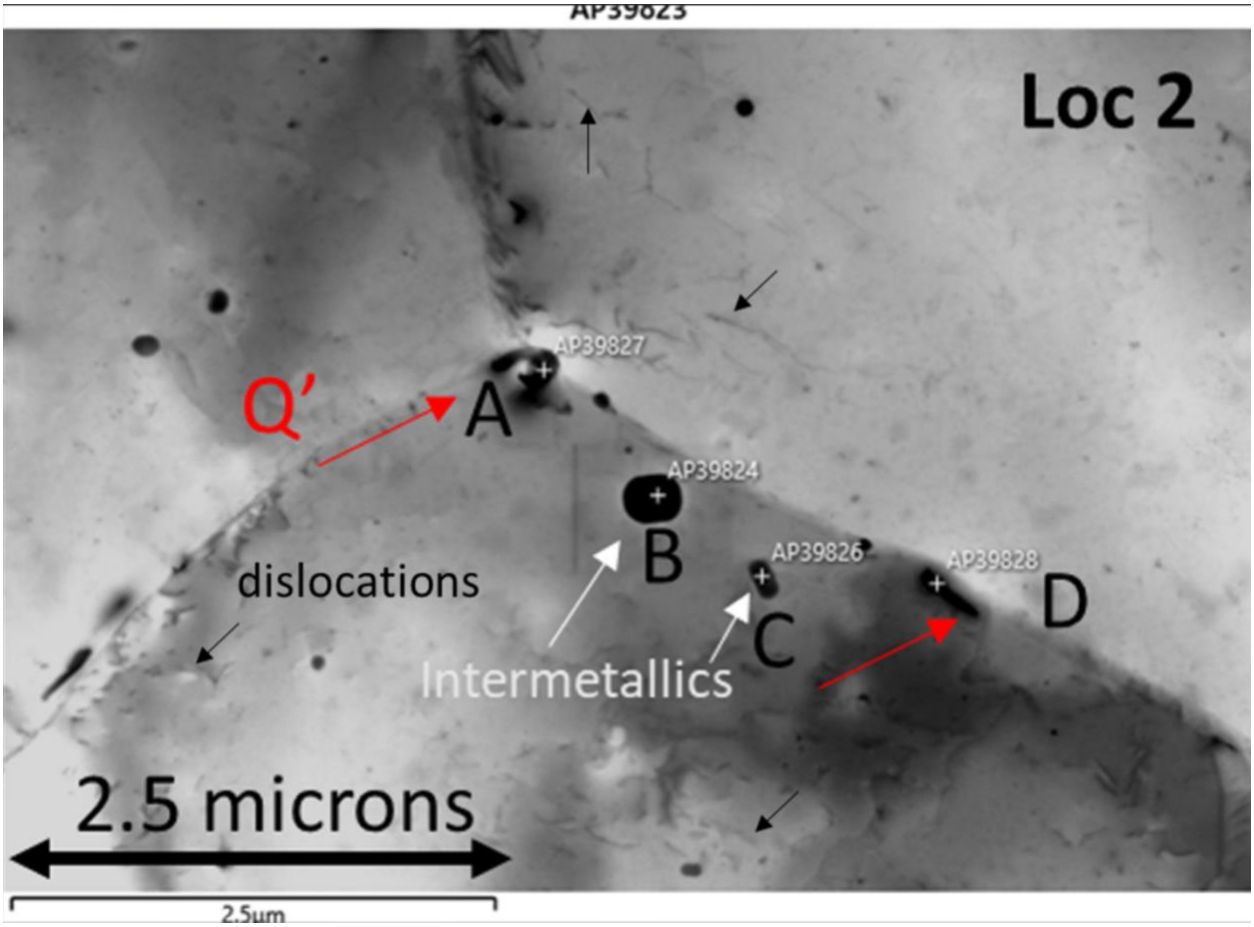
AP39623
Loc 2
AP39827
Q'
A
AP39824
B
AP39826
AP39828
D
dislocations
C
Intermetallics
2.5 microns
2.5um

Vote for your favorite entry here!

https://forms.office.com/r/0ZyzxCeUfT